molecules

MDPI

Article

Bioactive Compounds in *Ziziphus jujuba* Mill. Pulp/Peel and Stone: An Integrated Analytical Characterization

Francesca Sabatini [1,2,*], Matteo Di Berardino [1], Veronica Termopoli [1,2] and Heiko Lange [1,2,3]

[1] Department of Earth and Environmental Sciences, University of Milano-Bicocca, Piazza della Scienza 1, 20126 Milan, Italy; m.diberardino2@campus.unimib.it (M.D.B.); veronica.termopoli@unimib.it (V.T.); heiko.lange@unimib.it (H.L.)
[2] NBFC—National Biodiversity Future Centre, 90133 Palermo, Italy
[3] Biochemical Process Engineering, Division of Chemical Engineering, Department of Civil, Environmental and Natural Resources Engineering, Luleå University of Technology, SE-971 87 Luleå, Sweden
* Correspondence: francesca.sabatini@unimib.it

Abstract

Ziziphus jujuba Mill., *Rhamnaceae* family, is an Asian native fruit of nutritional and phytochemical interest. This study applied a multi-analytical approach combining headspace solid-phase microextraction, pyrolysis, and gas and liquid chromatography coupled by mass spectrometry (HS-SPME-GC-MS, GC-MS, Py-GC-MS, HPLC-MS), together with infrared, UV-visible, and phosphorus 31 nuclear magnetic resonance spectroscopy (ATR-FTIR, UV-Vis, ^{31}P NMR), to investigate the molecular profile of pulp/peel and stone (consisting of woody endocarp and the enclosed seed) fractions. The results revealed marked differences in chemical composition and extraction behavior. Pulp/peel, mainly characterized by a saccharide composition, is also rich in bioactive and volatile compounds, including terpenes, phenolic acids, flavonoids and anthocyanins, responsible for the red color. The stone is mainly lipidic, with a high content of polyphenols, compatible with hydrolysable tannins, and a lignocellulosic matrix. The combined chromatographic and spectroscopic results showed the different accessibility of these chemical fractions depending on the extraction strategy selected, highlighting the complementarity of different solvent extractions and thermal analysis. Overall, the study provides an integrated chemical characterization of *Ziziphus jujube* fractions, highlighting the potentiality of specific and separated future valorization strategies.

Keywords: *Ziziphus Jujuba*; bioactive compounds; anthocyanins; lignocellulosic materials; elemental content

Check for updates

Academic Editor: Claudio Ferrante

Received: 14 October 2026
Revised: 13 November 2026
Accepted: 23 November 2026
Published: 27 November 2026

Copyright: © 2026 by the authors. Licensee MDPI, Basel, Switzerland. This article is an open access article distributed under the terms and conditions of the Creative Commons Attribution (CC BY) license.

1. Introduction

Ziziphus jujuba Mill. is a deciduous fruit tree belonging to the *Rhamnaceae* family and is one of the most widely cultivated species of the genus *Ziziphus* [1]. The species is native to regions of South and East Asia, particularly China, India, Nepal and Pakistan, but it is currently cultivated in several other regions, including southern Europe [1,2]. The tree can reach 5–10 m in height and produces small greenish flowers during the summer, followed by fruits that ripen mainly between late summer and autumn [1,2]. The fruit is a drupe characterized by a pulp and a hard wood endocarp containing the seed. Depending on cultivar and ripening stage, the skin may range from yellow-green to reddish-brown. Jujube has a long history of cultivation and it has been used both as food and as a traditional medicinal resource [1].

Jujube has attracted increasing scientific interest because of its nutritional and phytochemical composition. The fruit contains carbohydrates, lipids, vitamins and minerals, together with several classes of secondary metabolites with potential biological activity as polyphenols [1,3]. These compounds have been associated with its antioxidant and anti-inflammatory properties. Nevertheless, its chemical composition can vary according to different *Ziziphus* species, cultivar, geographical origin, ripening stage and the selected analytical procedures [1,3–6].

From the perspective of chemical recovery and valorization, the jujube fruit can be considered as a heterogeneous rich matrix. The edible part, constituted by pulp and peel, and the stone differ considerably in composition and may thus provide different classes of compounds and opportunities for valorization [7]. Previous studies have reported phenolic compounds and flavonoids in the fruit tissues, whereas the stone has been mainly associated with lipophilic compounds, polysaccharides and tannin-rich fractions [1,3,8–10]. Recovery of these classes of compounds is also strongly dependent on the extraction strategy. Several procedures have been applied, including conventional solvent extraction, ultrasound-assisted extraction (UAE), microwave-assisted extraction (MAE) and headspace solid-phase microextraction (HS-SPME) using different solvents and conditions according to the target compounds [5,6,9–13]. Combined extraction strategies have been also explored to improve the recovery of selected bioactive compounds [9,10]. The application of liquid chromatography coupled by high-resolution mass spectrometry (LC-HRMS) has further expanded the characterization of jujube polar and phenolic constituents showing changes in pigment composition during fruit development in different jujube genera [13,14].

Despite the extensive information available on jujube composition, previous studies have generally focused on selected fruit fractions, compound classes or extraction procedures. An approach integrating different extraction strategies with complementary analytical techniques and widening jujube characterization from extractable compounds to its structural plant matrix is still missing.

In this study, a complementary multi-analytical approach has been applied to the pulp, peel and stone of *Z. jujuba* to investigate their chemical composition and the compounds accessible through different extraction procedures by gas chromatography–mass spectrometry (GC-MS). For pulp/peel, HS-SPME-GC-MS has been used to investigate its volatile fraction. High-performance liquid chromatography coupled with diode-array detection (HPLC-DAD) and HPLC-HRMS have been used to investigate pigments and polar compounds. Inductively coupled plasma optical emission spectrometry (ICP-OES) and graphite furnace atomic absorption spectroscopy (GF-AAS) have been employed to describe the elemental composition and reveal potentially toxic elements. Attenuated total reflectance Fourier transform infrared spectroscopy (ATR-FTIR), ^{31}P nuclear magnetic resonance (^{31}P NMR) spectroscopy and UV-Vis spectrophotometric assays have provided complementary information on polyphenolic fractions. Moreover, pyrolysis gas chromatography coupled by mass spectrometry (Py-GC-MS) has been applied to investigate thermally released compounds of polymeric fractions. For stone, the acid-soluble and acid-insoluble lignin and ash content have also been assessed. Overall, the study aimed to assess how the different fruit fractions and extraction approaches influence the chemical profile accessible from jujube and to identify their specific bioactive compounds for future valorization.

2. Results and Discussion

To comprehensively describe the composition of *Ziziphus jujuba*, the analytical workflow (Figure S1, Supplementary Materials) has been tailored to the specific characteristics of the fruit fractions. For the pulp and peel, the investigation was primarily focused on profiling the primary and secondary metabolites, including solvent-extractable organic compounds,

volatile constituents, polar species, pigments, and elemental composition. Conversely, the stone, due to its complex lignocellulosic nature, required adequate sequential extraction strategies and complementary approaches to isolate its phenolic content and assess its polymeric composition. Spectroscopic analyses have been additionally applied to both fractions to provide orthogonal information on their overall molecular composition and antioxidant characteristics.

2.1. Solvent Extraction and GC-MS Profiling of Pulp/Peel and Stone

The extraction procedures have been first compared to assess how solvent polarity and extraction conditions affected the chemical profiles obtained from jujube pulp and peel. In the preliminary UAE screening, acetone, methanol and dichloromethane/methanol (2:1, *v*/*v*) have produced richer chromatographic profiles in terms of the number and relative intensity of detected signals with respect to ethyl acetate, pure dichloromethane and hexane (Figure S2, Supplementary Materials). Therefore, they have been selected for the subsequent extraction experiments. Using methanol as an extraction solvent, Soxhlet, UAE and MAE have produced qualitatively similar GC-MS profiles, although differences in the relative abundance and chromatographic resolution of several compounds have been observed (Figure 1a). Chromatograms are mainly characterized by carbohydrate derivatives, as expected; organic acids, possibly responsible for the acidic taste; phenolic compounds; and a lower contribution from fatty acids (Table S1, Supplementary Materials). Furfural (**#1**), 2,4-dihydroxy-2,5-dimethyl-3(2*H*)-furanone (**#4**) and 5-hydroxymethylfurfural (**#12**), together with D-allose (**#14**) and quinic acid (**#19**), were among the recurrent constituents. Higher normalized peak areas were observed for the first three selected compounds in the UAE extracts compared with the Soxhlet extracts, with MAE giving intermediate values. Nevertheless, these differences provide a semi-quantitative indication of the compounds detected under each protocol rather than a direct measurement of extraction efficiency. They reflect the combined effect of the extraction procedure and the specific experimental conditions adopted and cannot be attributed to the extraction technique alone. Some differences were also observed in chromatographic resolution, particularly for D-allose (**#14**), levoglucosan (**#13**) and quinic acid (**#19**), whose signals are better resolved in the UAE chromatogram (Figure 1a).

The extraction behavior of the stone was widely different. Sequential Soxhlet and UAE extraction with dichloromethane, ethanol/toluene (1:1, *v*/*v*) and acetone, followed by the analysis of the corresponding extracts by GC-MS, provided profiles that differed substantially according to solvent polarity (Figure 1b; Table 1). The DCM extracts show the highest intense peaks above all the steps, dominated by low-polar compounds as fatty acids, particularly linoleic acid as a principal compound and palmitic acids. The ethanol/toluene fractions show a more differentiated composition, combining carbohydrate derivatives with phenolic and aromatic compounds such as gallic acid and pyrogallol. The acetone fractions are the least informative, mainly constituted by fatty acids. Comparison of the corresponding Soxhlet and UAE extracts further showed that the distribution of individual compounds depended on both solvent and extraction sequence, with compounds recovered in one step being less abundant or absent in subsequent fractions (Table 1).

The gravimetric extraction yields differed among the investigated procedures (US 51.5 ± 2.3 vs. Soxhlet 9.9% ± 0.8. for DCM, 11.7 ± 0.6 vs. 9.9 ± 0.9% for ethanol/toluene and 11.4 ± 0.7 vs. 0.7 ± 0.1% for acetone). Nevertheless, since the sample-over-solvent ratios, extraction times and operating conditions were not equivalent, these values are reported as yields dependent on the protocol and cannot be used to establish a direct comparison of extraction efficiency between Soxhlet and UAE. Moreover, differences in normalized

chromatographic areas are considered indicative of the chemical profiles obtained under the selected conditions rather than as absolute differences in compound recovery.

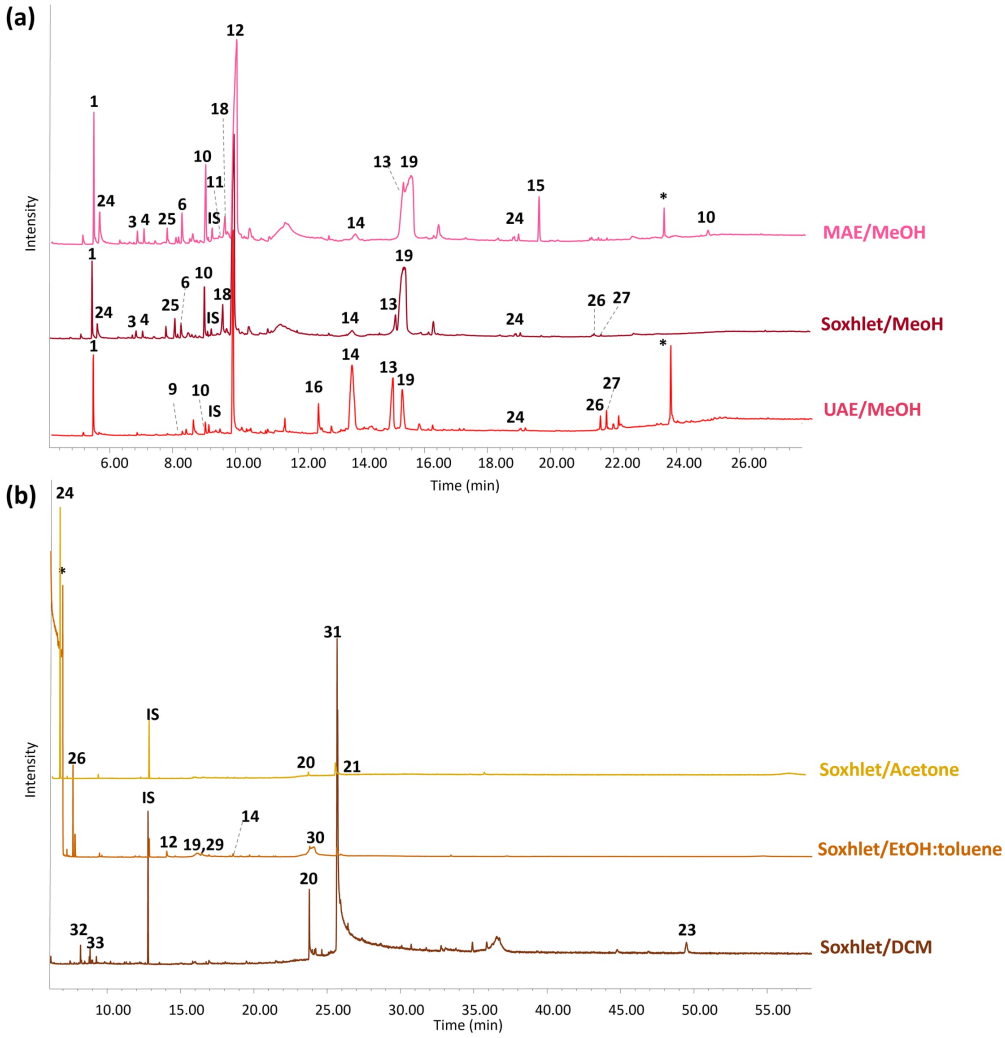

Figure 1. GC-MS chromatograms of (**a**) jujube pulp/peel Soxhlet/MeOH, UAE/MeOH, and MAE/MeOH extracts; (**b**) jujube stone Soxhlet/DCM, Soxhlet/EtOH:toluene, and Soxhlet/acetone extracts. All chromatograms are presented in the same scale and are stacked for purposes of clarity. IS: internal standard (cyclodecane). * Contaminants.

Overall, the extraction behavior differed between the two fractions. For pulp/peel, the three methanolic extractions provided largely overlapping profiles but differed in the relative recovery and chromatographic resolution. In contrast, the sequential extraction of the stone provided complementary profiles according to solvent polarity, allowing a more selective recovery of distinct chemical classes.

Table 1. List of compounds identified by GC-MS in jujube stone extracts obtained by different extraction procedures. The compounds are classified into distinct groups and ordered by increasing retention time within each class. The experimental linear retention indices (LRI_E) are compared with literature values (LRI_L) reported for non-polar stationary phases of similar composition, when available (n.a. = not available). For derivatized compounds, literature indices refer to the corresponding trimethylsilyl (TMS) derivatives are considered.

		LRI_E	LRI_L	Soxhlet			UAE		
				DCM	EtOH:Toluene	Acetone	DCM	EtOH:Toluene	Acetone
#	**Compounds**								
	Furanic and carbohydrate derivatives								
12	5-Hydroxymethylfurfural (TMS)	920	n.a.		X				
14	D-Allose (5TMS)	1022	n.a.		X				
	Other aromatic and phenolic compounds								
26	Ethylbenzene	872	858		X				
27	Benzaldehyde	971	959–962					X	
28	Benzyl alcohol (TMS)	1143	1150–1153					X	
29	Pyrogallol (3TMS)	1574	1560–1562	X	X		X	X	
18	*p*-Coumaraldehyde (TMS)	1601	n.a.				X		
30	Gallic acid (4TMS)	1958	1979		X				
	Organic acids								
19	Malic acid (3TMS)	1490	1497		X				
	Fatty acids								
20	Palmitic acid (TMS)	2030	2040–2050	X		X	X	X	
31	Linoleic acid (TMS)	2117	n.a.	X	X	X	X	X	
21	Oleic acid (TMS)	2201	2216			X	X	X	
22	Stearic acid (TMS)	2218	2234				X		
	Tocopherols								
23	α-Tocopherol (TMS)	3166	3156	X					
	Other organic compounds								
24	4-Hydroxy-4-methyl-2-pentanone (TMS)	751	n.a.	X		X		X	
32	3-Methyl-2-butenal	520	n.a.						
33	1-Methyl-2-propylcyclohexane	948	n.a.	X					

2.2. HS-SPME-GC-MS Characterization of Volatile Compounds

HS-SPME-GC-MS provided a complementary chemical window into jujube pulp/peel to that obtained by solvent extraction. While the latter chromatographic profiles are largely characterized by carbohydrate derivatives and fatty acids, the HS-SPME analysis led to the tentative identification of 10 compounds (library match scores ranging from 88% to 96%) belonging to four chemical classes, with terpenes representing the largest group in terms of the number of identifications (Figure S3 and Table S2, Supplementary Materials). Linalool (**#39**) and (*E*)-geranylacetone (**#40**) have been already reported for *Z. jujuba* [13,14], while farnesol (**#41**), kaur-15-ene (**#42**) and kaur-16-ene (**#43**) have not been found before in this drupe. Aldehydes as nonanal (**#36**) and decanal (**#37**) together with as methyl palmitate (**#38**) are also consistent with volatiles documented for this fruit [13,14].

Overall, HS-SPME-GC-MS provided a description of the volatile fraction of pulp/peel, highlighting its terpenoid components, which were not detected in the solvent-extractable fraction (Table S1, Supplementary Materials).

2.3. HPLC-DAD and HPLC-HRMS Characterization of Polar Compounds and Pigments

HPLC-DAD and HPLC-HRMS have been used to characterize the polar fraction of jujube pulp/peel, with particular focus on phenolic compounds and dyes. The HPLC-DAD chromatogram (Figure S4, Supplementary Materials) shows two peaks whose UV-vis spectrum displays an absorption maximum at 505 nm and 516 nm, respectively. The spectral profiles are characterized by the typical absorption of anthocyanins, generally observed around 510–520 nm, together with a shoulder in the 400–450 nm region [15]. The position and shape of the visible absorption are also influenced by the hydroxylation pattern of the anthocyanidin moiety, with pelargonidin- and cyanidin-based compounds showing characteristic differences in their absorption maxima [15]. Based on the UV-vis spectrum, the combination of the retention time and the accurate mass obtained by HPLC-HRMS, the two peaks have been ascribed to cyanidin 3-*O*-glucoside (m/z = 449.109) and pelargonidin-3-*O*-glucoside (m/z = 433.114), respectively.

Moreover, HPLC-HRMS widely expands the chemical profile, allowing us to identify 17 compounds ranging from phenolic acids, flavonoids and flavonol derivatives to proanthocyanidin compounds and anthocyanins (Table 2). Among phenolic acids, gallic acid (**#30**), caffeic acid (**#44**), protocatechuic acid (**#45**), syringic acid (**#46**), p-coumaric acid (**#47**) and vanillic acid (**#48**) have been detected. Gallic acid has already been identified by GC-MS in the stone, whereas the further phenolic acids have not been observed in the GC-MS profiles. The occurrences of gallic, protocatechuic and caffeic acids were already reported as constituents of phenolic fraction of jujube fruit [16,17], yet the present work provides a broader overview and adds information on this aspect.

The flavonoid fraction included both aglycones and glycosylated derivatives. Kaempferol-*O*-hexoside (**#49**), quercetin (**#54**), kaempferol-3-*O*-rutinoside/kaempferol-3-*O*-neohesperidoside (**#50**), quercetin-3-*O*-rutinoside (rutin, **#51**), quercetin-*O*-hexoside isomers (**#53**) and kaempferol (**#52**) have been detected, together with a procyanidin B2-type dimer (**#55**), in accordance with the literature [17,18]. At the same time, the combination of aglycones, *O*-glycosylated derivatives and a proanthocyanidindime emphasizes the chemical heterogeneity of the polar fraction investigated here. For the glycosylated flavonoids, the exact positional and/or stereochemical configuration of isomeric structures cannot be established unambiguously from the present dataset.

The anthocyanin fraction entails cyanidin-3-*O*-glucoside (**#56**), cyanidin 3-*O*-rutinoside (**#57**), pelargonidin-3-*O*-glucoside (**#58**) and cyanidin (**#59**). The detection of these compounds provides molecular support for the red coloring compounds [19,20] observed by HPLC-DAD and links the visible spectral response to anthocyanin pigments present in the

fruit matrix. In particular, the presence of glycosylated anthocyanins indicates that the red pigment fraction is represented predominantly by conjugated forms rather than only by the corresponding aglycones.

Table 2. List of compounds identified by HPLC-HRMS in jujube pulp/peel, classified into distinct groups. The molecular formula, retention time (RT), precursor ion, mass error (ppm), and MS/MS product ions are reported. For each compound, only the ion form selected for assignment is listed. A dash indicates that no product ions were detected under the applied MS/MS conditions.

#	Compound	Molecular Formula	Rt (min)	Ion Adducts (ESI+/ESI−)	Precursor Ion (ESI+/ESI−)	Mass Error (ppm)	Product ions (MS/MS)
	Phenolic acids						
30	Gallic acid	$C_7H_6O_5$	1.22	$[M-H]^-$	169.014	5.9	125.024, 107.014
44	Caffeic acid	$C_9H_8O_4$	6.56	$[M-H]^-$	179.035	5.6	135.045
45	Protocatechuic acid	$C_7H_6O_4$	7.24	$[M-H]^-$	153.018	4.6	109.028
46	Syringic acid	$C_9H_{10}O_5$	7.66	$[M-H]^-$	197.045	5.1	182.020, 166.997, 123.007
47	*p*-Coumaric acid	$C_9H_8O_3$	7.79	$[M-H]^-$	163.040	4.9	119.050
48	Vanillic acid	$C_8H_8O_4$	7.98	$[M-H]^-$	167.035	3.6	152.0124, 108.022
	Flavonoids and flavonol derivatives						
49	Kaempferol-*O*-hexoside (astragalin)	$C_{21}H_{20}O_{11}$	7.26	$[M+H]^+$	449.108	−1.0	287.054
50	Kaempferol-3-*O*-rutinoside (nicotiflorin)/kaempferol-3-*O*-neohesperidoside	$C_{27}H_{30}O_{15}$	7.53	$[M+H]^+$	595.165	−1.7	449.107, 287.055
51	Quercetin-3-*O*-rutinoside (rutin)	$C_{27}H_{30}O_{16}$	8.81	$[M-H]^-$	609.147	1.9	301.004
52	Kaempferol	$C_{15}H_{10}O_6$	8.33	$[M+H]^+$	287.055	−0.6	153.017, 121.028
53	Quercetin-*O*-hexoside isomers (isoquercitrin/hyperoside)	$C_{21}H_{20}O_{12}$	9.31	$[M-H]^-$	463.089	2.6	301.004, 271.023, 255.026
54	Quercetin	$C_{15}H_{10}O_7$	12.03	$[M-H]^-$	301.035	0.7	179.004, 151.007
	Proanthocyanidins						
55	Procyanidin B2-type dimer (tentatively assigned as procyanidin B2)	$C_{30}H_{26}O_{12}$		$[M-H]^-$	577.135	0.62	425.084, 407.076, 289.071
	Anthocyanins						
56	Cyanidin-3-*O*-glucoside	$C_{21}H_{21}O_{11}^+$	7.27	M^+	449.109	−1.0	287.055
57	Cyanidin 3-*O*-rutinoside	$C_{27}H_{31}O_{15}^+$	7.52	M^+	595.164	−2.3	287.055
58	Pelargonidin-3-*O*-glucoside	$C_{21}H_{21}O_{10}^+$	7.72	M^+	433.114	−0.81	271.060
59	Cyanidin	$C_{15}H_{11}O_6^+$	8.33	M^+	287.054	-0.6	-

Overall, the HPLC-DAD-HRMS analysis describes a different chemical portion of pulp/peel, rich in phenolic acids, flavonoids and anthocyanins, not accessible through GC-MS treatment and analysis. Therefore, the combined use of chromatographic approaches extended the characterization from extractable low-molecular-weight compounds to less volatile and more polar constituents.

2.4. Characterization of Phenolic and Tannin Fractions by FTIR, UV-Vis and ^{31}P NMR Spectroscopy

ATR-FTIR spectroscopy allowed us to describe the changes occurring in the main functional group osf the two matrices after solvent extractions. The solid residues after Soxhlet/acetone extraction and after aqueous extraction were considered, respectively, for pulp/peel and stone (Figure 2a,b). In the lyophilized pulp, the broad band centered at approximately 3300 cm^{-1}, associated with O–H stretching, shows a lower absorption after Soxhlet extraction, consistently with the removal of part of the fraction containing hydroxyl groups. Additional bands at 1726–1710 cm^{-1}, 1603 cm^{-1} and around 1020 cm^{-1} are associated with carbonyl and conjugated C=C and C–O vibrations, respectively, reflecting

the coexistence of oxygenated, phenolic and carbohydrate components in the fruit [21,22]. The differences between the spectra collected before and after extraction indicate that the solvent treatment selectively removed some components of the matrix, resulting in changes in the relative intensity of the corresponding bands.

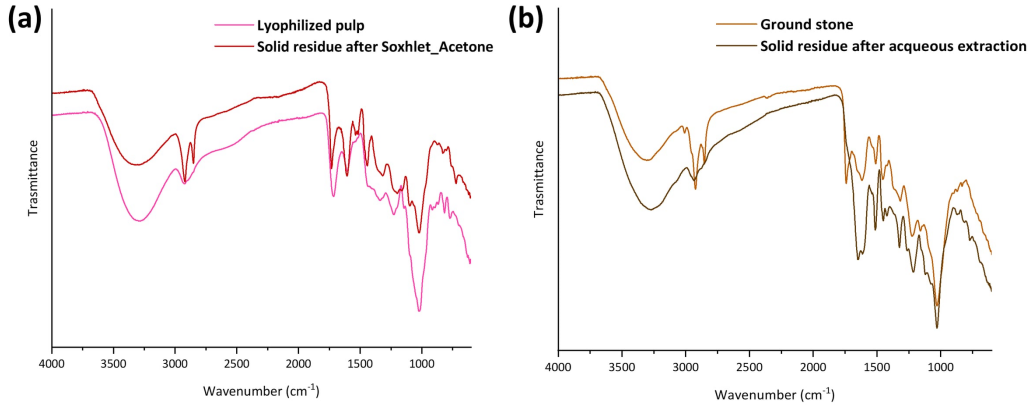

Figure 2. ATR-FTIR spectra of (**a**) jujube freez-dried pulp/peel and the respective solid residue after Soxhlet/acetone extraction; (**b**) jujube ground stone and the respective solid residue after aqueous extraction.

The spectral changes are more pronounced in the stone. The untreated material shows distinct bands at 2922 and 2848 cm^{-1}, ascribable to aliphatic C–H stretching and consistent with the lipid fraction previously evidenced by GC-MS (Table 1). These bands are strongly attenuated after the sequential extraction procedure, indicating a relevant decrease in lipid components. Conversely, the bands at 1643, 1510 and 1322 cm^{-1} become more evident in the extraction residue. These signals are compatible with the presence of aromatic and oxygenated structures, including phenolic components, although they are not specific to any particular tannin class [23]. The persistence of an intense OH band in the residue further supports the presence of compounds rich in hydroxyl groups, in agreement with the spectrophotometric results.

The Folin–Ciocalteu assay gives a total phenolic content (TPC) of 106.8 ± 0.2 mg GAE/g for the pulp/peel and 412.5 ± 0.0 mg GAE/g for the stone. For the first, the obtained value is within the range previously reported for *Z. jujuba*, although differences among cultivars, tissues and extraction procedures have been described [24]. The higher response of the stone indicates a greater reducing capacity towards the Folin–Ciocalteu reagent, although this assay provides a global response and does not distinguish among individual phenolic classes. Differences between the two matrices bee also reflected by the Scalbert assay: the response is 0.499 ± 0.005 mg CyaE/g for pulp/peel, while it is only 0.012 ± 0.000 mg CyaE/g for stone. The substantially lower response of the stone suggests a limited contribution of condensed tannins/proanthocyanidins, although the assay response alone does not allow their unequivocal quantification or the identification of other tannin classes. In contrast, several anthocyanins are identified in the pulp/peel by HPLC-HRMS.

Indeed, ^{31}P NMR analysis provided further insight into the hydroxyl group distribution of the stone residue after aqueous extraction (Figure S5, Supplementary Materials). Signals attributable to aliphatic OH groups (3.45 mmol/g) are observed in the 148–145 ppm region, and aromatic OH groups (1.38 mmol/g) are observed between 141 and 137 ppm, including the region at 138–137 ppm associated with p-hydroxyphenyl groups, while those between 135 and 133 ppm are ascribable to carboxylic acid OH group (0.71 mmol/g) [25]. The predominance of aliphatic over aromatic hydroxyl groups indicates a heterogeneous hydroxyl fraction rather than one dominated by aromatic phenolic structures. Together with

the low response in the Scalbert assay and the detection of gallic acid by GC-MS (Table 1), these findings are compatible with the presence of phenolic components potentially associated with hydrolysable tannins, although neither FTIR nor ^{31}P NMR could provide their unequivocal occurrence.

2.5. Lignin Content and Py-GC-MS Characterization of the Structural Fraction

Py-GC-MS has been applied to investigate the molecular profile of pulp/peel and stone, further marking the respective differences between the two polymeric matrices (Figure 3 and Table 3). To the best of our knowledge, no previous Py-GC-MS studies have been performed on *Ziziphus jujube*. The analysis was performed at 550 °C, and the resulting profiles were interpreted qualitatively, focusing on the chemical families of the detected products rather than on the relative abundance of individual structural units.

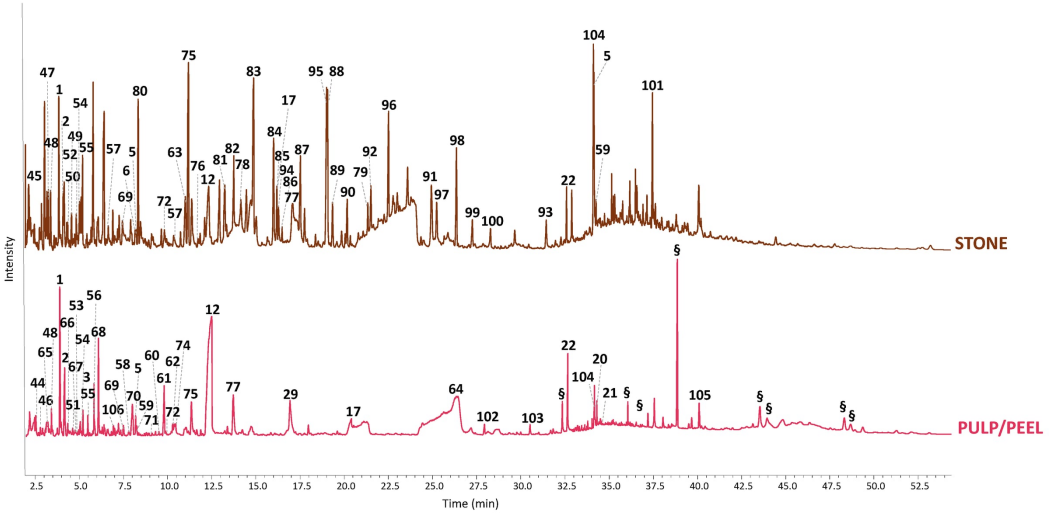

Figure 3. Py-GC-MS pyrograms of jujube stone and pulp/peel. The two pyrograms are presented in the same scale and are stacked for purposes of clarity. § Linear hydrocarbons.

Table 3. List of compounds identified by Py-GC-MS in jujube stone and pulp/peel. The table provides a qualitative overview of the detected compounds, with "X" indicating their presence in the respective matrix. The assignments are based on mass spectral library comparisons, and no quantitative comparison of individual compounds is intended. The compounds are classified into distinct groups and ordered by increasing retention time within each class.

#	Compounds	Stone	Pulp
	Furanic and carbohydrate-derivatives		
44	2,5-Dimethylfuran		X
45	Methyl acetate	X	
46	2,3-Butanedione		X
47	Succinaldehyde	X	
48	5-(Hydroxymethyl)-2(5*H*)-furanone	X	X
1	Furfural	X	X
2	Maleic anhydride	X	X
49	Furfuryl alcohol	X	
50	5-Methyl-2(3*H*)-furanone	X	
51	2-Cyclopentene-1,4-dione		X
52	5,6-Dihydro-2*H*-pyran-2-one	X	
53	2-Methyl-2-cyclopentenone		X
54	2(5*H*)-Furanone	X	X
55	1,2-Cyclopentanedione	X	X
56	Methylmaleic anhydride		X

Table 3. *Cont.*

#	Compounds	Stone	Pulp
3	5-Methyl-2-furaldehyde		X
57	2-Hydroxy-1-methylcyclopenten-3-one	X	
58	2-Furancarboxylic acid		X
5	1-(2-Furanyl)-2-hydroxyethanone	X	X
6	Methyl 2-furoate	X	
59	2,5-Dimethylfuran-3,4(2*H*,5*H*)-dione		X
60	Maltol		X
61	3,5-Dihydroxy-6-methyl-2,3-dihydro-4*H*-pyran-4-one		X
62	Dehydromevalonic lactone		X
63	Hydroxymaltol	X	
12	5-Hydroxymethylfurfural	X	X
64	Carbohydrate-derived pyrolysis products		X
	Other aromatic and phenolic compounds		
65	Toluene		X
66	Xylene		X
67	Styrene		X
68	Phenol		X
69	2-Cresol	X	X
70	5-Methylresorcinol		X
71	2-Methylbenzofuran		X
72	2,5-Dimethylphenol	X	X
73	2,3-Dihydroxybenzaldehyde	X	
74	Benzoic acid		X
75	Catechol	X	X
76	3-Vinylphenol	X	
77	Hydroquinone	X	X
78	3-Methyl-pyrocatechol	X	
29	Pyrogallol	X	X
17	3-Hydroxybenzoic acid		X
79	Resorcinol	X	
	Guaiacyl-derivatives		
80	Guaiacol	X	
81	3-Methoxy-1,2-benzenediol	X	
82	*p*-Ethylguaiacol	X	
83	2-Methoxy-4-vinylphenol	X	
84	Syringol	X	
85	Eugenol	X	
86	5-Propylguaiacol	X	
87	Vanillin	X	
88	Isoeugenol	X	
89	*p*-Propylguaiacol	X	
90	Apocynin	X	
91	Homovanillic acid	X	
92	Guaiacylacetone	X	
93	5-(3-Hydroxypropyl)-2,3-dimethoxyphenol	X	
	Syringyl-derivatives		
94	3,4-Dimethoxyphenol	X	
95	3,5-Dimethoxy-4-hydroxytoluene	X	
96	2,6-Dimethoxy-4-vinylphenol	X	
97	Syringaldehyde	X	
98	2,6-Dimethoxy-4-(prop-1-en-1-yl)phenol	X	
99	Acetosyringone	X	
100	Syringylacetone	X	
101	3,3′-Dimethoxy-4,4′-dihydroxystilbene	X	
	Fatty acids and other lipid compounds		
102	Myristic acid		X
103	Pentadecanoic acid		X
104	Linoelaidic acid	X	X
20	Palmitic acid	X	

Table 3. *Cont.*

#	Compounds	Stone	Pulp
21	Oleic acid	X	X
22	Stearic acid	X	X
105	3,5-Cholestadiene		X
	Terpenes		
106	Limonene		X

The pulp/peel pyrogram is mainly characterized by compounds eluting at low retention times ascribable to carbohydrate thermal degradation. Furfural (**#1**), 3,5-dihydroxy-6-methyl-2,3-dihydro-4*H*-pyran-4-one (**#61**) and 5-hydroxymethylfurfural (**#12**) are among the most intense peaks, following by other several furanones, pyranones and cyclopentantnes. These compounds are consistent with cellulose and hemicellulose thermal degradation products reported for plants and fruits [26,27]. In particular, furans and anhydrosugar products are commonly associated with cellulose degradation, whereas hemicellulose can contribute to the formation of smaller oxygenated compounds, including furans, aldehydes and organic acids [27,28]. Interestingly, several of the compounds detected by Py-GC-MS as furfural (**#1**), maleic anhydride (**#2**), 5-methyl-2-furaldehyde (**#3**), 1-(2-furanyl)-2-hydroxyethanone (**#5**), 5-hydroxymethylfurfural (**#12**) and fatty acids are also identified in the respective extracts analyzed by GC-MS (Table S1, Supplementary Materials). This correspondence shows that some compounds already accessible in the pulp/peel matrix and are also generated during pyrolysis of its structural components, although the two approaches provide different information on their molecular origin. The prevalence of furanic and oxygenated products in the pyrogram supports a substantial contribution of carbohydrate components to the structural fraction, in agreement with pyrolysis profiles reported for cellulose and other lignocellulosic materials [26,29,30].

The stone pyrogram shows a more complex aromatic profile still characterized by carbohydrate derivatives but with a broad distribution of intense aromatic and phenolic compounds at intermediate retention times. This region is thus characterized by numerous phenolic products, with particularly prominent signals associated with methoxylated phenols and aldehydes. Guaiacol (**#80**), 2-methoxy-4-vinylphenol (**#83**) and vanillin (**#87**) are detected among the guaiacyl-derived products, while syringol (**#84**), syringaldehyde (**#97**) and acetosyringone (**#99**) represent characteristic syringyl ones. Guaiacylacetone (**#92**) and syringylacetone (**#100**) further contribute to this pattern. The occurrence of several products associated with both guaiacyl and syringyl units is consistent with the presence of lignin structure in the woody endocarp and seed-containing fraction, as commonly observed for angiosperm seed lignins [31]. The aromatic profile also includes catechol (**#75**), 3-methyl-pyrocatechol (**#78**) and pyrogallol (**#29**) generated by the thermal degradation of different phenolic structures present in the polyphenolic fraction. In particular, pyrogallol, detected in both matrices, can be formed by the thermal decarboxylation of gallic acid, and it is also a product reported in the pyrolysis of hydrolysable tannins to distinguish from condensed ones [32,33], potentially providing additional information on the phenolic composition of the stone. The simultaneous detection of carbohydrate and lignin products indicates the coexistence of polysaccharide and aromatic structural components in the stone matrix [34]. Fatty acids are also highly relevant in the latter part of the pyrogram, in agreement with the GC-MS profile (Table 1), where these compounds represent a major part of the extractable lipid fraction of the stone.

The high acid-insoluble residue measured by the Klason method is 37.8% of the dry stone, which, together with the comparatively low acid-soluble fraction (0.5%), indicates a substantial acid-insoluble structural fraction. The ash content determined on the untreated ground is 1.58 ± 0.04%, indicating a relatively low inorganic fraction, accordingly with

values reported for jujube stones [35]. The occurrence of several guaiacyl and syringyl compounds detected by Py-GC-MS supports the presence of lignin-related structures in the stone. Nevertheless, the Klason values obtained should be interpreted with attention: acid-insoluble residues from lignocellulosic matrices may contain other non-lignin components such as suberin, protein and tannin-derived materials. Similarly, acid-soluble lignin could be also constituted by hydrolysable tannins preferentially transferred in this fraction during acid hydrolysis [32]. Therefore, although the combined results support the occurrence of lignin in the stone, its actual contribution to the total Klason residue cannot be quantitatively established.

The spectroscopic and spectrophotometric results indicate marked differences in the phenolic fraction of pulp/peel and stone. In the former, the phenolic profile is characterized by anthocyanins and flavonoids identified by HPLC-HRMS (Table 2), whereas the latter shows a high TPC but a very low Scalbert response, suggesting a limited contribution of condensed tannins/proanthocyanidins. The ^{31}P NMR data (Figure S5) provides information on the distribution of hydroxyl groups, while the detection of gallic acid and pyrogallol by GC-MS and Py-GC-MS, respectively, is compatible with the occurrence of galloyl-containing phenolic compounds, potentially including hydrolysable tannins [36,37].

2.6. Elemental Composition and Trace Metal Assessment

The elemental composition and heavy metal assessment of the pulp/peel has been performed by ICP-OES, while GF-AAS has been only used for arsenic and lead determination (Table 4). Potassium is the most abundant element (1532.4 µg/g), followed by calcium (278.4 µg/g) and magnesium (100.32 µg/g). This distribution is in accordance with the elemental profile reported for *Z. jujube*, although significant differences have been described among cultivars, growing conditions and harvesting periods [1,38]. Aluminum and sodium are detected at 8.00 and 6.48 µg/g, respectively, while iron and zinc are present at 3.20 and 1.24 µg/g. Manganese, copper and nickel occur at trace levels, while heavy metals such as chromium, cadmium, arsenic and lead were below the detection limits (LOD) of the ICP-OES method. Arsenic and lead were not detected by GF-AAS, with concentrations below the corresponding LOD of 0.0025 µg/g in the original dry sample.

Table 4. Elemental composition of jujube pulp/peel. Concentrations are expressed as µg/g dry weight. All the elements were determined by ICP-OES except for As and Pb, which were assessed by GF-AAS. n.d. = not detected (below the corresponding LOD).

Element	Concentration (µg/g)
Potassium (K)	1532.40
Calcium (Ca)	278.40
Magnesium (Mg)	100.32
Aluminum (Al)	8.00
Sodium (Na)	6.48
Iron (Fe)	3.20
Zinc (Zn)	1.24
Copper (Cu)	0.56
Manganese (Mn)	0.32
Nickel (Ni)	0.040
Chromium (Cr)	n.d.
Cadmium (Cd)	n.d.
Arsenic (As)	n.d.
Lead (Pb)	n.d.

3. Materials and Methods

3.1. Chemicals and Materials

The solvents and reagents used for sample pretreatments are the following: dichloromethane (DCM; GC-MS grade, Merck KGaA, Darmstadt, Germany), acetone (HPLC grade, VWR Chemicals, Milan, Italy), ethyl acetate (AcOEt; HPLC grade, Carlo Erba, Milan, Italy), methanol (MeOH; LC-MS grade, Carlo Erba, Milan, Italy), ethanol (EtOH; purity ≥ 99.8%, Sigma-Aldrich, St. Louis, MO, USA), toluene (purity ≥ 99.5%, Sigma-Aldrich, St. Louis, MO, USA), magnesium sulfate ($MgSO_4$; purity ≥ 97%, Merck KGaA, Darmstadt, Germany), sodium chloride (NaCl; ACS grade, Merck KGaA, Darmstadt, Germany), nitric acid (HNO_3; Sigma-Aldrich, St. Louis, MO, USA), and hydrogen peroxide (H_2O_2; ACS grade, Merck KGaA, Darmstadt, Germany). Ultra-pure Milli-Q water was employed in the preparation steps.

For the GC-MS silanization reaction *N*,*O*-bis(trimethylsilyl)trifluoroacetamide with 1% trymethylclorosilane (BSTFA + 1% TMCS; purity ≥ 97%, Merck KGaA, Darmstadt, Germany) and pyridine (py; 99.8% purity, Merck KgaA, Darmstadt, Germany) were used. To monitor the analytical response and normalize chromatographic signals, geraniol (purity 98%, Merck KgaA, Darmstadt, Germany) at 2.5 ppm in ethanol was used as the internal standard for the HS-SPME-GC-MS procedure while cyclodecane (purity ≥ 90%, Merck KGaA, Darmstadt, Germany) at 200 ppm in AcOEt was chosen for GC-MS. A C7–C40 saturated alkane mixture (certified reference material, Merck KGaA, Darmstadt, Germany) at 10 ppm hexane was used to calculate linear retention indices (LRIs).

The eluents used for HPLC-DAD and HPLC-HRMS analysis were formic acid (FA; 98–100% purity, Sigma Aldrich, St. Louis, MO, USA), water, and acetonitrile at HPLC grade (Sigma Aldrich, St. Louis, MO, USA) and LC-MS grade (Sigma Aldrich, St. Louis, MO, USA) for HPLC-DAD and HPLC-HRMS analysis, respectively. PTFE filters (pore size 0.45 µm) were used for extract filtration.

For the UV-vis spectrophotometric tests, Folin–Ciocalteau (Merck KGaA, Darmstadt, Germany) 10% in water solution and sodium carbonate (Na_2CO_3; purity ≥ 99.5%, Sigma-Aldrich, St. Louis, MO, USA), 7.5% (*w*/*w*) aqueous solution, and gallic acid (ACS reagent grade, ≥98.0%, Merck KGaA, Darmstadt, Germany) for calibration were used; while for the Scalbert test, iron(II) sulphate heptahydrate ($FeSO_4 \cdot 7\ H_2O$; purity ≥ 99%, Riedel-de Haen, Seelze, Germany) in hydrochloric acid (HCl; purity 37%, Sigma-AldrichSt. Louis, MO, USA) and isobutanol (purity ≥ 99.5%, Carlo Erba, Milan, Italy) (2:3) were employed.

For the ^{31}P NMR analysis, Cr(III) acetylacetonate ($Cr(acac)_3$; Fluorochem, Hadfield, Derbyshire, UK) dissolved in py and deuterated chloroform ($CDCl_3$; 99.8 atom % D, Merck KGaA, Darmstadt, Germany) solution (1.6:1 *v*/*v*), *exo*-*N*-hydroxy-5-norbornene-2,3-dicarboximide (*e*-HNDI; Fluorochem, Hadfield, Derbyshire, UK) as the internal standard and 2-chloro-4,4,5,5-tetramethyl-1,3,2-dioxaphospholane (Cl-TMDP; purity≥ 97%, Sigma-Aldrich, St. Louis, MO, USA) as the phosphitylating agent were used.

Ziziphus jujuba fruits (approximately 100 g in total), visually assessed as ripe, were collected in October 2023 at Parco della Besozza (Pioltello, Milan, Italy), located near an industrial area. The cultivar was not available. The collected fruits were treated as a single pooled sample and were not intended to represent biological variability among different trees or cultivars. After washing the fruits under running tap water, the pulp and peel were manually separated from the hard inner part of the fruit (stone, consisting of woody endocarp and the enclosed seed), and the two fractions were stored at -18 °C. Subsequently, the pulp and peels were freeze-dried using a LIO-5P lyophilizer (Cinquepascal S.r.l., Milan, Italy) for about 72 h and then manually ground into a fine powder. The entire hard fraction, including both the endocarp and seed, was mechanically pulverized. Unless otherwise stated, all subsequent analyses were performed using these sample forms (referred to as

freeze-dried pulp/peel and **ground stone**). All analytical determinations reported in triplicate were performed on three aliquots of the same homogenized sample. Results are expressed as mean ± standard deviation (SD). These measurements represent analytical replicates and do not correspond to independent biological samples.

3.2. Extraction Procedures

Freeze-dried pulp/peel and ground stone were subjected to Soxhlet extraction, ultrasound-assisted extraction (UAE), and microwave-assisted extraction (MAE) prior to subsequent analytical determinations, including GC-MS and ^{31}P NMR. The measurements were performed on three aliquots of the same homogenized sample for both pulp/peel and stone. A procedural blank was analyzed under the same conditions for all extraction methods, and background peaks were excluded prior to compound identification.

Soxhlet Extraction:

- *Freeze-dried pulp/peel*: Approximately 5 g of sample was extracted with 150 mL of MeOH (8 h, heat block at 80 °C). An aliquot was saved for GC-MS analyses, while the remainder was evaporated to dryness and weighed to determine extraction yield.
- *Ground stone:* Approximately 5 g of sample was extracted sequentially using 150 mL of the following solvents: DCM (4 h, heat block at 60 °C), EtOH:toluene 1:1 (v/v, 8 h, heat block at 160 °C), and acetone (8 h, heat block at 60 °C). Each extraction was performed under reflux. After each step, an aliquot was collected for GC-MS analysis, the remaining solution was evaporated to dryness for yield determination, and the solid residue was dried before proceeding to the next solvent. Following the sequential Soxhlet extractions, the final solid residue was extracted with 150 mL of distilled water for 8 h under reflux, using a heating-block setting at 120 °C to recover water-soluble components, such as polyphenols, for ^{31}P NMR characterization. The extract was centrifuged, and the collected supernatant was freeze-dried for 48 h.

Ultrasound-Assisted Extraction (UAE): extractions were carried out using an ultrasonic bath (Super RK 512 H Sonorex, Bandelin Electronic, Berlin, Germany; 120 W, 35 kHz) at 30 °C for 30 min.

- *Freeze-dried pulp/peel:* Approximately 30 mg of sample was extracted in 2 mL of solvent (acetone, MeOH, DCM, or MeOH:DCM 2:1 v/v). The liquid phase was dried over $MgSO_4$, filtered, and analyzed by GC-MS.
- *Ground stones:* Approximately 30 mg of sample was extracted in 2 mL of solvent (DCM, ethanol:toluene 1:1 (v/v), or acetone). To enable direct comparison with Soxhlet extractions, a sequential extraction was also performed using the same solvent order (DCM → ethanol:toluene 1:1 v/v → acetone); after each step, the liquid phase was evaporated to dryness for yield calculation, and the dried residue was extracted with the next solvent. All extracts were dried over $MgSO_4$ and filtered.

Microwave-Assisted Extraction (MAE): Extraction was performed using a Multiwave 5000 extractor equipped with a Rotor 16HF100 (Anton Paar GMbH, Graz, Austria). Approximately 0.6 g of freeze-dried pulp was extracted in 6 mL of MeOH (liquid-to-solid ratio 1:10 m/v) at 182 W for a total of 30 min. The temperature was ramped from 25 °C to 65 °C over 10 min (4 °C/min) and held at 65 °C for 20 min.

Summarizing, the solvent-to-sample ratios differed among the extraction procedures, being 30 mL/g for Soxhlet extraction, 66.7 mL/g for UAE and 10 mL/g for MAE. These differences, together with the different extraction times and temperatures, should be considered when interpreting the chromatographic profiles.

3.3. Gas Chromatography Coupled with Mass Spectrometry (GC-MS)

To an aliquot (500 µL) of the extracts collected by the pretreatments described in Section 3.5, 10 µL cyclodecane (200 ppm in ethyl acetate) was added as an internal standard and subjected to silanizant derivatization using 15 µL of BSTFA + 1% TMCS and 15 µL of py (RT for 30 min). Linear retention indices (LRIs) were calculated according to the literature [39] by injecting a standard mixture of *n*-alkanes (C7–C40, 10 ppm in hexane) under the corresponding GC temperature programs used for sample analyses. The experimental LRIs were calculated by interpolation between the retention times of the n-alkanes eluting immediately before and after each compound. Experimental LRIs were compared with literature values reported for non-polar capillary columns with similar stationary phase composition. For derivatized compounds, literature values referring to the corresponding TMS derivatives were considered whenever available.

The analysis was performed with a Shimadzu GCMS-QP2020NX (Shimadzu Corporation, Kyoto, Japan). An SH-Rxi-5ms fused silica capillary column (stationary phase (5%-phenyl)-methylpolysiloxane, 30 m × 0.25 mm i.d., 0.25 µm, Shimadzu Corporation, Kyoto, Japan) was used for chromatographic separation. The injection volume was 1 µL and the injection port operated at 280 °C in splitless mode. The helium flow was kept constant at 1 mL/min (carrier gas, purity 99.995%). Chromatographic separation was performed using two matrix-specific oven temperature programs. For freeze-dried pulp/peel, the oven temperature was held at 50 °C for initial thermal equilibrium, ramped by 20 °C/min to 150 °C (held for 1 min), increased by 10 °C/min to 250 °C (held for 3 min), and finally raised by 30 °C/min to 310 °C (held for 6 min), giving a total run time of 28 min. For ground stone, the oven temperature was held at 60 °C, ramped by 10 °C/min to 280 °C, and held isothermally for 33 min, resulting in a total run time of 58 min. The MS transfer line was kept at 280 °C while the ion source and quadrupole temperature were kept at 230 °C and 150 °C, respectively. The MS operated in electron ionization mode (EI) at 70 eV, in positive mode scanning in the range from 35 to 500 m/z. LabSolutions–GCMS Version 4.54 software (Shimadzu Corporation, Kyoto, Japan) was used for system control, instrument management, and data acquisition. Substances were identified using NIST MS Search, version 2.4 (2020) (National Institute of Standards and Technology, Gaithersburg, MD, USA) and only components exhibiting a match value of greater than 800 were included. Chromatographic peak areas were normalized (A_{norm}) according to the following equation:

$$A_{norm} = A_{compound}/(A_{IS} \times m_{dry})$$

where $A_{compound}$ is the peak area of the target analyte, A_{IS} is the peak area of the internal standard (cyclodecane), and m_{dry} is the sample dry weight (in grams).

3.4. Headspace Solid-Phase Micro Extraction Coupled with Gas Chromatography and Mass Spectrometry (HS-SPME-GC-MS)

An amount of 30 mg of freeze-dried pulp/peel, 20 µL of a standard solution of geraniol at 2.5 ppm (Internal Standard, IS), and 1 g of NaCl were mixed in 8 mL of water into 20 mL headspace screw vials, equipped with polytetrafluorethylene-silicone septa. The solution was continuously stirred at 200 rpm with a magnetic bar and incubated for 10 min at 60 °C to establish temperature equilibrium. Subsequently, an SPME fiber (50/30 µm DVB/CAR/PDMS, 1 cm long; Supelco, Palo Alto, CA , USA), previously conditioned as recommended by the manufacturer, was inserted into the sample head space and left to sample the volatile fraction for 30 min at the same temperature of incubation. The fiber was then withdrawn from the vial and immediately introduced into the GC-MS injector for the desorption step at 240 °C for 3 min. The measurements were performed on three aliquots of the same homogenized samples. A procedural blank was analyzed under the

same conditions, and background peaks originating from the SPME fiber or sample vials were excluded prior to compound identification.

The same GC-MS instrument described in Section 3.3. was used. Also, the analytical column, MS parameters and data management employed were retained. The injection port operated in splitless mode, and the purge flow to split vent was 7 mL/min at 3 min. The following chromatographic program was used: starting temperature 45 °C, then 10 °C/min to 60 °C, 15 °C/min to 200 °C, 20 °C/min to 230 °C, then hold for 6 min.

3.5. Pyrolysis Coupled with Gas Chromatography and Mass Spectrometry (Py-GC-MS)

About 200 µg of freeze-dried pulp and ground stones were placed into a separated clean stainless-steel cup and the cup was inserted into a microfurnace. The measurements were performed on three aliquots of the same homogenized samples both for pulp/peel and ground stone.

An EGA/PY-3030D microfurnace pyrolyzer (Frontier Laboratories Ltd., Fukushima, JP) coupled to the same GC-MS instrument described in Section 3.3 was used. Also, the analytical column, MS parameters and data management employed were retained.

The pyrolysis time for each shot was 0.2 s and the pyrolysis temperature was 550 °C. The injection port operated at 280 °C, with a 10:1 split ratio, and the interface temperature was kept at 280 °C. The pyrolysis products were eluted in constant flow mode using helium (1 mL/min) as a carrier gas. The chromatographic program was as follows: 50 °C isothermal for 1 min; 10 °C/min up to 100 °C, then isothermal for 2 min; 4 °C/min up to 190 °C, then isothermal for 1 min; 30 °C/min up to 280 °C, then isothermal for 20 min.

3.6. High-Performance Liquid Chromatography Coupled to Diode Array Detector (HPLC-DAD) and High-Resolution Mass Spectrometry (HPLC-HRMS)

An amount 0.1 mg of freeze-dried pulp/peel was dissolved in 1 mL of methanol and ultrasonicated for 30 min at 60 °C (ultrasonic bath Sonorex Supra 10P, Bandelin Electronics, Berlin, Germany). Then, it was filtered with a PTFE filter, and an injection volume of 10 µL and 4 µL was selected for HPLC-DAD and HPLC-HRMS, respectively.

The HPLC-DAD system consists of a PU-2089 quaternary pump equipped with a degasser, an AS-950 autosampler, and an MD-2010 spectrophotometric diode array detector. All the modules were Jasco International Co. (Tokyo, Japan). The DAD detector operated with spectral acquisition ranging from 200 to 650 nm every 0.2 s, with a resolution of 4 nm. Data acquisition and analysis were performed using ChromNav software (Jasco International Co., Tokyo, Japan).

The HPLC-ESI-Q-ToF is made of an HPLC 1200 Infinity coupled to a Jet Stream ESI-Q-ToF 6530 Infinity detector with an Agilent Infinity autosampler (Agilent Technologies, Palo Alto, CA, USA). The mass spectrometer operated in ESI ionization **in negative and positive mode**, and the working conditions were as follows: drying gas N_2 (purity > 98%) temperature, 350 °C and 10 L/min flow; capillary voltage, 4.5 KV; nebulizer gas pressure, 35 psig; sheath gas temperature, 375 °C and 11 L/min flow; fragmentor voltage, 175 V. High-resolution MS and MS/MS spectra were acquired in the range 100–1700 m/z at a scan rate of 1.04 spectra/sec (CID voltage 30 V, collision gas N_2, purity 99.999%). Auto-calibration was performed daily using Agilent tuning mix HP0321 (Agilent Technologies) prepared in acetonitrile. MassHunter® Workstation Software (B.10.00) was used to carry out mass spectrometer control, data acquisition, and data analysis.

The chromatographic separation was performed on an analytical reversed-phase column Poroshell 120 EC-C18 (3.0 × 75 mm, particle size 2.7 µm) equipped with an InfinityLab Poroshell 120 EC-C18 guard-column (3.0 × 5.0 mm, particle size 2.7 µm), both Agilent Technologies (Palo Alto, CA, USA). The eluents were A, formic acid (FA 0.1% v/v) in

LC-MS grade water, and B, formic acid (FA 0.1% *v*/*v*) in LC-MS grade acetonitrile. The flow rate was 0.4 mL/min. The program was 5% B for 2.6 min, then to 50% B in 13.0 min, to 70% B in 5.2 min, to 100% B in 6.2 min and then hold for 8.0 min; re-equilibration took 11 min. During the separation, the column was thermostated at 30 °C.

3.7. Attenuated Total Reflection Fourier Transform Infrared Spectroscopy (ATR-FT-IR)

A few grains of freeze-dried pulp/peel and ground stone were analyzed by ATR-FT-IR. Spectra were acquired with a Nicolet iS10 spectrometer (Thermo Fisher Scientific, Waltham, MA, USA) equipped with a diamond iTR Smart device (total scan 32, range 4000–600 cm^{-1}, resolution 4 cm^{-1}). OMNIC spectra (Thermo Fisher Scientific, Waltham, MA, USA) was used for data acquisition.

3.8. UV-Vis Spectrophotometric Tests

For freeze-dried pulp/peel and ground stone, total phenolic content (Folin-Cicalteu test) and proanthocyanidin activity (Scalbert test) were evaluated measuring absorbance value by a V-730 UV-visible/NIR double-beam spectrophotometer (Jasco Europe S.r.l., Lecco, Italy) with a halogen and a deuterium lamp, a single monochromator and a silicon photodiode detector. A scanning speed of 8000 nm/min was used for full spectrum acquisition, with a range of 190–1100 nm and resolution of 0.1 nm. Spectra were acquired and processed with Spectra Manager 2.5 Suite Spectroscopy Software (Jasco Europe S.r.l., Lecco, Italy). All measurements were performed on three aliquots of the same homogenized sample, and the results are expressed as the mean.

Folin–Ciocalteu test [40]: The Folin–Ciocalteu reagent was diluted 1:10 in deionized water. A solution was prepared by simultaneously adding 1.25 mL of the reagent and 0.25 mL of a sample solution in distilled water with a concentration of about 0.5 mg/mL. After 2 min, the solution was buffered with 1 mL aqueous solution of sodium carbonate (Na_2CO_3) 7.5% (*m*/*m*), resulting in a sample dilution factor (d) of 10. The mixture was heated at 50 °C for 5 min in an oven, and then the absorbance was read at $\lambda = 765$ nm. A calibration curve was obtained following this approach using a solution of gallic acid in distilled water (0.5 mg/mL). The total phenolic content (TPC) or mg of gallic acid (GAE) equivalent per g of dry sample was calculated as follows:

$$\text{TPC (mg GAE/g sample)} = \text{C (mg GAE/mL)} \times \text{V}_{\text{tot}} \text{ (mL)/m (g)}$$

where C is the gallic acid equivalent concentration obtained from the calibration curve, V_{tot} is the total volume of the sample solution, and m is the mass of dry sample analyzed (g).

Scalbert test [41]*:* The Scalbert reagent was prepared by dissolving 38.5 mg of $FeSO_4 \cdot 7H_2O$ in 250 mL of an HCl:isobutanol mixture in a 2:3 (*v*/*v*) ratio. Then, 5.0 mL of the reagent was added to 0.5 mL the sample solution already prepared for the Folin–Ciocalteu test, resulting in a sample dilution factor (d) of 11. The mixture was heated at 95 °C for 15 min in an oven. Absorbance was read at $\lambda = 530$ nm. Results were expressed in cyanidin equivalents (CyaE) as mg per g of dry tannin (mg CyaE/g tannin) according to the following equation:

$$\text{mg CyaE/g tannin} = (\text{A} \times \text{V} \times \text{d} \times \text{MM} \times 1000)/(\varepsilon \times \text{l} \times \text{m})$$

where A is absorbance, V is the total reaction volume (mL), d is the dilution factor, MM is the molar mass of cyanidin (287.24 g/mol), ε is the molar extinction coefficient of cyanidin (3.47×10^4 L/mol·cm), l is the optical path length (1 cm), and m is the mass of the analyzed sample (g).

3.9. Phosphorus 31 Nuclear Magnetic Resonance Spectroscopy (^{31}P NMR)

The analysis was performed exclusively on ground stone solid residual obtained at the end of the aqueous extraction (Section 3.2). An amount of c.a. 10 mg of this sample was dissolved in 425 µL of a 0.01 M solution of $Cr(acac)_3$ in a pyridine and deuterated chloroform ($CDCl_3$) mixture at a volume ratio of 1.6:1 v/v. To this, 100 µL of a 0.1 M solution of *e*-HNDI in a pyridine/$CDCl_3$ mixture (also at a 1.6:1 v/v ratio) was added as an internal standard. The solution was stirred vigorously for two hours before adding 75 µL of 2 Cl-TMPD to complete the phosphitylation process for about 60 min at room temperature. The prepared mixture was then transferred to a 5 mm NMR tube for analysis.

The ^{31}P NMR spectra were acquired using a Bruker 400 MHz spectrometer (Billerica, MA, USA). The temperature of the probe was maintained at 20 °C and the inversed gated decoupling technique was applied. For quantitative analysis, the spectral settings included a 90° pulse width and a sweep width of 6600 Hz. A 15 s delay was implemented between successive pulses to accumulate the spectra. A line broadening factor of 4 Hz was applied, and drift correction was carried out before performing the Fourier transform.

3.10. Determination of Acid-Insoluble and -Soluble Lignin (Klason Lignin)

For the determination of acid-insoluble lignin, approximately 100 mg of ground stone was carefully weighed into a test tube. To this, 2 mL of 72% (m/m) sulfuric acid solution was added at room temperature, with intermittent stirring over a 2 h period. The resulting solution was then diluted with deionized water to achieve a 3% (m/m) sulfuric acid concentration. Then, the solution was transferred to a sealed flask and subjected to heating at 121 °C and 2 atm for 1 h using a pressure cooker. The solution was filtered through a crucible of size M and washed with deionized water until a neutral pH was attained, and the crucibles were placed in an oven at 105 °C overnight to fully dry the sample. The acid-insoluble lignin was determined gravimetrically.

For the assessment of acid-soluble lignin, the filtrate obtained from the acid-insoluble lignin procedure was diluted to 100 mL using deionized water. The quantification was performed by calculating UV absorbance at 205 nm, using the same UV-Vis spectrometer and the same operating conditions previously described, utilizing an extinction factor of 113 L/g·cm, chosen according to the literature for hardwoods [42].

3.11. Ash Content

The ash content of lignin of ground stone was defined as the residue remaining after ignition at 650 °C for 4 h, providing the measure of mineral salts in the lignin [43]. The measurement was performed on three aliquots of the same homogenized sample, and the result is expressed as the mean.

3.12. Inductively Coupled Plasma Atomic Emission Spectroscopy (ICP-OES)

An amount of 200 mg of freeze-dried pulp/peel was placed in a PTFE vessel and digested with the same microwave extractor described in Section 3.5, by adding 5 mL of 65% (m/m) HNO_3 65% and 2 mL 40% H_2O_2 in a closed system to reduce the risk of contamination. The system was programmed to reach 230 °C in 30 min; the temperature was maintained for 15 min and then cooled down to room temperature in 45 min. After digestion, samples were diluted to a final volume of 10 mL. A procedural blank was prepared using the same reagents and digestion procedure, without the addition of the sample.

An aliquot of the diluted digested sample was analyzed by an ICP OES Optima 7000 DV (Perkin Elmer Inc., Waltham, MA, USA) system. Calibration curves for each target element were generated automatically by the software (WinLab32) (Perkin Elmer Inc., Waltham, MA, USA) using three-level standard solutions prepared in 2% (m/m) HNO_3.

Blank (2% (*m*/*m*) HNO_3) and sample measurements were performed at the following specific emission wavelengths: Fe (259.939 nm), Cr (267.716 nm), Zn (206.200 nm), Cu (224.700 nm), Ni (231.604 nm), Cd (214.440 nm), Mn (257.610 nm), Ca (393.366 nm), K (766.490 nm), Na (589.592 nm), Mg (280.271 nm), and Al (396.152 nm). Samples for Ca, K, Mg, and Al analysis were diluted 1:10 (*v*/*v*) with Milli-Q water prior to measurement.

3.13. Graphite Furnace Atomic Absorption Spectroscopy (GF-AAS)

Another aliquot of the diluted digested sample, prepared as explained in Section 3.12, was analyzed by a GF-AAS AAnalyst 600 (Perkin Elmer Inc., Waltham, USA) system. GF-AAS was used for the determination of lead and arsenic, given its higher sensitivity with respect to ICP-OES, useful to detect elements in traces as could be the case for these highly toxic metals, if present. Calibration curves for As and Pb were automatically constructed (WinLab32) by autosampler-driven serial dilutions of a 50 ppb stock standard solution in 0.2% (*m*/*m*) HNO_3. Blank (0.2% (*m*/*m*) HNO_3), standard, and sample measurements were performed following the addition of an equal volume of matrix modifier to each solution. Analysis was carried out under element-specific operating conditions: As was determined at 193.7 nm using a matrix modifiers of 0.005 mg Pd + 0.003 mg $Mg(NO_3)_2$, with pyrolysis and atomization temperatures of 1200 °C and 2000 °C, respectively; Pb was measured at 238.2 nm using 0.05 mg of $NH_4H_2PO_4$ and 0.003 mg of $Mg(NO_3)_2$ as matrix modifiers, with pyrolysis and atomization temperatures of 850 °C and 1500 °C, respectively. The limit of detection (LOD) was 0.05 ppb for both elements in the analytical solution, corresponding to 0.0025 µg/g in the original freeze-dried sample.

4. Conclusions

This combined chromatographic, spectroscopic and spectrometric study demonstrates that the potential of *Ziziphus jujuba* is closely related to the differentiated chemical composition of its edible pulp/peel and stone fraction, which could provide distinct valorization resources. While previous studies have investigated selected chemical classes or compared different jujube species, the present work integrates complementary profiling of solvent-extractable and volatile compounds with spectroscopic characterization and Py-GC-MS analysis of the structural fraction. To our knowledge, this study represents the first application of Py-GC-MS to *Ziziphus jujuba* characterization. In addition, HS-SPME-GC-MS provided tentative evidence for the occurrence of terpenes as farnesol, kaur-15-ene and kaur-16-ene in the fruit, which, to our knowledge, have not been previously reported in this matrix. The pulp/peel is characterized by a profile rich in bioactive compounds, including phenolic acids, flavonoids and anthocyanins, as well as a volatile portion constituted by terpenoids. The stone, in contrast, highlights a composition mainly made by lipids and a phenolic fraction compatible with hydrolysable tannins, while pyrolysis revealed a structural matrix constituted both by carbohydrates and lignin. The complementary analytical approaches also demonstrated that these components are accessed differently according to the extraction procedure used, supporting the choice of selective and sequential strategies rather than a single extraction step. The compositional differences suggest distinct but complementary valorization pathways for the two fractions. The pulp/peel, as the edible portion of the fruit, may represent a source of phytochemicals of interest for future food-related applications, including the development of ingredients enriched in phenolic compounds. The stone, generated as a by-product of fruit processing, represents a lignocellulosic biomass whose lipid, phenolic and structural fraction could be further investigated as potential feedstocks for bio-based applications and material development. Further studies addressing biological activity and application performance will be needed to assess these prospects.

Supplementary Materials: The following supporting information can be downloaded at https://www.mdpi.com/article/10.3390/molecules31234344/s1, Figure S1: Workflow relative to jujube pulp/peel and stone treatment and analysis; Figure S2: Comparison of the GC-MS profiles jujube pulp/peel UAE extracts collected using different solvents. All chromatograms are presented in the same scale and are stacked for purposes; Figure S3: HS-SPME-GC-MS chromatogram of the volatile fraction of jujube pulp/peel. IS: internal standard (geraniol); Figure S4: HPLC-DAD chromatogram extracted at maximum of absorbance 450–550 nm of jujube pulp/peel with the UV-Vis spectra of the identified compounds; Figure S5: ^{31}P NMR spectrum of the jujube stone residue after aqueous extraction; Table S1: List of compounds identified by GC-MS in all the jujube pulp/peel extracts obtained by different extraction procedures. The compounds are classified into distinct groups and ordered by increasing retention time within each class. The experimental linear retention indices (LRIE) are compared with literature values (LRIL) reported for non-polar stationary phases of similar composition, wherever available (n.a. = not available). For derivatized compounds, literature indices refer to the corresponding trimethylsilyl (TMS) derivatives are considered; Table S2: List of compounds tentatively identified by HS-SPME-GC-MS in the volatile fraction of jujube pulp/peel. Compounds are classified into chemical groups and retention time (RT) and match score (%) (similarity score obtained from mass spectral comparison with the NIST library) are reported for each of them.

Author Contributions: Conceptualization, F.S., V.T. and H.L.; methodology, F.S.; formal analysis, M.D.B. and F.S.; data curation, M.D.B., V.T. and F.S.; supervision, F.S.; writing—original draft, F.S. and M.D.B.; writing—review and editing, F.S., V.T. and H.L.; funding acquisition, H.L. All authors have read and agreed to the published version of the manuscript.

Funding: Project funded under the National Recovery and Resilience Plan (NRRP), Mission 4 Component 2 Investment 1.4—Call for tender No. 3138 of 16 December 2021, rectified by Decree n.3175 of 18 December 2021 of Italian Ministry of University and Research funded by the European Union—NextGenerationEU. Award Number: Project code CN_00000033, Concession Decree No. 1034 of 17 June 2022 adopted by the Italian Ministry of University and Research, CUP, H43C22000530001 Project title "National Biodiversity Future Center—NBFC".

Data Availability Statement: The data that support the findings of this study are available from the corresponding author (F.S.) upon reasonable request.

Acknowledgments: The authors would like to thank Ilaria Degano and Adele Ferretti from the Department of Chemistry and Industrial Chemistry of the University of Pisa, Italy, for preparing the samples and performing the HPLC-DAD and HPLC-HRMS analysis.

Conflicts of Interest: The authors declare no conflicts of interest.

References

1. Gao, Q.-H.; Wu, C.-S.; Wang, M. The Jujube (Ziziphus Jujuba Mill.) Fruit: A Review of Current Knowledge of Fruit Composition and Health Benefits. *J. Agric. Food Chem.* **2013**, *61*, 3351–3363. [CrossRef] [PubMed]
2. Roberts, J.; Dhileepan, K.; Florentine, S. A Review of the Biology, Distribution, and Management Challenges Posed by the Invasive Weed Ziziphus Mauritiana L., with Special Reference to Its Invasion in Australia. *Weed Res.* **2024**, *64*, 8–18. [CrossRef]
3. Zhu, J.; Lu, Y.; He, Q. Recent Advances on Bioactive Compounds, Health Benefits, and Potential Applications of Jujube (Ziziphus Jujuba Mill.): A Perspective of by-Products Valorization. *Trends Food Sci. Technol.* **2024**, *145*, 104368. [CrossRef]
4. Abd-Alrahman, S.H.; Salem-Bekhit, M.M.; Elhalwagy, M.E.A. Chemical Composition and Antimicrobial Activity of Ziziphus Jujuba Seed Extract. *J. Pure Appl. Microbiol.* **2013**, *7*, 379–385.
5. Al-Saeedi, A.H.; Al- Ghafri, M.T.H.; Hossain, M.A. Comparative Evaluation of Total Phenols, Flavonoids Content and Antioxidant Potential of Leaf and Fruit Extracts of Omani Ziziphus Jujuba L. *Pac. Sci. Rev. A Nat. Sci. Eng.* **2016**, *18*, 78–83. [CrossRef]
6. Kushwaha, P.; Yadav, S.S.; Singh, V.; Dwivedi, L.K. GC-MS Analysis of Bio-Active Compounds in Methanolic Extract of Ziziphus Mauritiana Fruit. *Int. J. Pharm. Sci. Res.* **2019**, *10*, 2911–2916. [CrossRef]
7. Chianese, A.; Mushtaq, H.; Nastri, B.M.; Morone, M.V.; Giugliano, R.; Khan, H.; Piccolella, S.; Zannella, C.; Pacifico, S.; Galdiero, M.; et al. Getting Insights into Chemical Composition and Antiherpetic Capability of Jujube (Ziziphus Jujuba Mill.) Drupes. *Heliyon* **2024**, *10*, e37037. [CrossRef] [PubMed]

8. Miklavčič Višnjevec, A.; Baruca Arbeiter, A.; Hladnik, M.; Ota, A.; Skrt, M.; Butinar, B.; Nečemer, M.; Krapac, M.; Ban, D.; Bučar-Miklavčič, M.; et al. An Integrated Characterization of Jujube (Ziziphus Jujuba Mill.) Grown in the North Adriatic Region. *Food Technol. Biotechnol.* **2019**, *57*, 17–28. [CrossRef] [PubMed]
9. Berkani, F.; Dahmoune, F.; Serralheiro, M.L.; Ressaissi, A.; Dairi, S.; Kadri, N.; Remini, H.; Abbou, A.; Madani, K. New Bioactive Constituents Characterized by LC–MS/MS in Optimized Microwave Extract of Jujube Seeds (Zizyphus Lotus L.). *J. Food Meas. Charact.* **2021**, *15*, 3216–3233. [CrossRef]
10. Wu, Z.; Li, H.; Wang, Y.; Yang, D.; Tan, H.; Zhan, Y.; Yang, Y.; Luo, Y.; Chen, G. Optimization Extraction, Structural Features and Antitumor Activity of Polysaccharides from Z. Jujuba Cv. Ruoqiangzao Seeds. *Int. J. Biol. Macromol.* **2019**, *135*, 1151–1161. [CrossRef] [PubMed]
11. Suzuki, M.; Wilkie, C.A. The Thermal Degradation of Acrylonitrile-Butadiene-Styrene Terpolymer as Studied by TGA/FTIR. *Polym. Degrad. Stab.* **1995**, *47*, 217–221. [CrossRef]
12. Zhu, J.; Kou, X.; Wu, C.; Fan, G.; Li, T.; Dou, J.; Shen, D. Enhanced Extraction of Bioactive Natural Products Using Ultrasound-Assisted Aqueous Two-Phase System: Application to Flavonoids Extraction from Jujube Peels. *Food Chem.* **2022**, *395*, 133530. [CrossRef] [PubMed]
13. Wang, L.; Wang, Y.; Wang, W.; Zheng, F.; Chen, F. Comparison of Volatile Compositions of 15 Different Varieties of Chinese Jujube (Ziziphus Jujuba Mill.). *J. Food Sci. Technol.* **2019**, *56*, 1631–1640. [CrossRef] [PubMed]
14. Liu, Y.; Sang, Y.; Guo, J.; Zhang, W.; Zhang, T.; Wang, H.; Cheng, S.; Chen, G. Analysis of Volatility Characteristics of Five Jujube Varieties in Xinjiang Province, China, by HS-SPME-GC/MS and E-nose. *Food Sci. Nutr.* **2021**, *9*, 6617–6626. [CrossRef] [PubMed]
15. Saha, S.; Singh, J.; Paul, A.; Sarkar, R.; Khan, Z.; Banerjee, K. Anthocyanin Profiling Using UV-Vis Spectroscopy and Liquid Chromatography Mass Spectrometry. *J. AOAC Int.* **2020**, *103*, 23–39. [CrossRef] [PubMed]
16. Xue, X.; Zhao, A.; Wang, Y.; Ren, H.; Du, J.; Li, D.; Li, Y. Composition and Content of Phenolic Acids and Flavonoids among the Different Varieties, Development Stages, and Tissues of Chinese Jujube (Ziziphus Jujuba Mill.). *PLoS ONE* **2021**, *16*, e0254058. [CrossRef] [PubMed]
17. Qin, S.; Yan, F.; E, S.; Xiong, P.; Tang, S.; Yu, K.; Zhang, M.; Cheng, Y.; Cai, W. Comprehensive Characterization of Multiple Components of Ziziphus Jujuba Mill Using UHPLC-Q-Exactive Orbitrap Mass Spectrometers. *Food Sci. Nutr.* **2022**, *10*, 4270–4295. [CrossRef] [PubMed]
18. Choi, S.-H.; Ahn, J.-B.; Kozukue, N.; Levin, C.E.; Friedman, M. Distribution of Free Amino Acids, Flavonoids, Total Phenolics, and Antioxidative Activities of Jujube (Ziziphus Jujuba) Fruits and Seeds Harvested from Plants Grown in Korea. *J. Agric. Food Chem.* **2011**, *59*, 6594–6604. [CrossRef] [PubMed]
19. Liu, H.; Wang, L.; Liu, H.; Deng, B.; Li, S.; Zhao, X. Quantification and Identification Analysis of Ziziphus Jujuba Mill. Peel Pigmentation at Different Developmental Stages. *Food Chem. X* **2022**, *16*, 100470. [CrossRef] [PubMed]
20. Shi, Q.; Du, J.; Zhu, D.; Li, X.; Li, X. Metabolomic and Transcriptomic Analyses of Anthocyanin Biosynthesis Mechanisms in the Color Mutant Ziziphus Jujuba Cv. Tailihong. *J. Agric. Food Chem.* **2020**, *68*, 15186–15198. [CrossRef] [PubMed]
21. Etika, S.B.; Iryani, I. Isolation and Characterization of Flavonoids from Black Glutinous Rice (Oryza Sativa L. Var Glutinosa). *Eksakta Berk. Ilm. Bid. MIPA* **2019**, *20*, 6–16. [CrossRef] [PubMed]
22. Jeyaram, S.; Geethakrishnan, T. Vibrational Spectroscopic, Linear and Nonlinear Optical Characteristics of Anthocyanin Extracted from Blueberry. *Results Opt.* **2020**, *1*, 100010. [CrossRef]
23. Falcão, L.; Araújo, M.E.M. Tannins Characterization in Historic Leathers by Complementary Analytical Techniques ATR-FTIR, UV-Vis and Chemical Tests. *J. Cult. Herit.* **2013**, *14*, 499–508. [CrossRef]
24. Xue, Z.; Feng, W.; Cao, J.; Cao, D.; Jiang, W. Antioxidant Activity and Total Phenolic Contents in Peel and Pulp of Chinese Jujube (Ziziphus jujuba Mill) Fruits. *J. Food Biochem.* **2009**, *33*, 613–629. [CrossRef]
25. Meng, X.; Crestini, C.; Ben, H.; Hao, N.; Pu, Y.; Ragauskas, A.J.; Argyropoulos, D.S. Determination of Hydroxyl Groups in Biorefinery Resources via Quantitative 31P NMR Spectroscopy. *Nat. Protoc.* **2019**, *14*, 2627–2647. [CrossRef] [PubMed]
26. Mattonai, M.; Tamburini, D.; Colombini, M.P.; Ribechini, E. Timing in Analytical Pyrolysis: Py(HMDS)-GC/MS of Glucose and Cellulose Using Online Micro Reaction Sampler. *Anal. Chem.* **2016**, *88*, 9318–9325. [CrossRef] [PubMed]
27. Carrier, M.; Windt, M.; Ziegler, B.; Appelt, J.; Saake, B.; Meier, D.; Bridgwater, A. Quantitative Insights into the Fast Pyrolysis of Extracted Cellulose, Hemicelluloses, and Lignin. *ChemSusChem* **2017**, *10*, 3212–3224. [CrossRef] [PubMed]
28. Galletti, G.C.; Reeves, J.B. Pyrolysis/Gas Chromatography/Ion-Trap Detection of Polyphenols (Vegetable Tannins): Preliminary Results. *Org. Mass Spectrom.* **1992**, *27*, 226–230. [CrossRef]
29. Nardella, F.; Mattonai, M.; Andreozzi, F.; Betrò, M.; Ribechini, E. Long-Lasting Flavor Compounds of Myrtle and Immortelle from Ancient Egyptian Tombs: A Study by Analytical Pyrolysis. *J. Anal. Appl. Pyrolysis* **2024**, *177*, 106305. [CrossRef]
30. Hao, J.; Xu, F.; Yang, D.; Wang, B.; Qiao, Y.; Tian, Y. Analytical Pyrolysis of Biomass Using Pyrolysis-Gas Chromatography/Mass Spectrometry. *Renew. Sustain. Energy Rev.* **2025**, *208*, 115090. [CrossRef]

31. Tobimatsu, Y.; Chen, F.; Nakashima, J.; Escamilla-Treviño, L.L.; Jackson, L.; Dixon, R.A.; Ralph, J. Coexistence but Independent Biosynthesis of Catechyl and Guaiacyl/Syringyl Lignin Polymers in Seed Coats. *Plant Cell* **2013**, *25*, 2587–2600. [CrossRef] [PubMed]
32. Bunzel, M.; Schüssler, A.; Saha, G.T. Chemical Characterization of Klason Lignin Preparations from Plant-Based Foods. *J. Agric. Food Chem.* **2011**, *59*, 12506–12513. [CrossRef] [PubMed]
33. Sabatini, F.; Mattonai, M.; Doherty, B.; Degano, I. Unveiling the Composition of Native Asian Dye Plants by EGA/MS and Py-GC/MS. *J. Anal. Appl. Pyrolysis* **2025**, *186*, 106979. [CrossRef]
34. Monção, M.; Thoresen, P.P.; Wretborn, T.; Lange, H.; Rova, U.; Christakopoulos, P.; Matsakas, L. A Novel Biorefinery Concept Based on Marginally Used Halophyte Biomass. *Sustain. Energy Fuels* **2023**, *7*, 3902–3918. [CrossRef]
35. Jyoti, A.; Gunjal, M.; Rasane, P.; Gaur, S.S.; Ercisli, S.; Singh, J. Characterization of Ziziphus Jujuba Seeds and Optimization of Waffle Formulations via D-Optimal Mixture Design. *Sustain. Food Technol.* **2026**, *4*, 3061–3078. [CrossRef]
36. Ferretti, A.; Sabatini, F.; Degano, I. Linking Historical Recipes and Ageing Mechanisms: The Issue of 19th Century Iron Gall Inks. *J. Cult. Herit.* **2024**, *67*, 111–120. [CrossRef]
37. Ferretti, A.; Sabatini, F.; Degano, I. A Model Iron Gall Ink: An In-Depth Study of Ageing Processes Involving Gallic Acid. *Molecules* **2022**, *27*, 8603. [CrossRef] [PubMed]
38. Fukalova Fukalova, T.; García-Martínez, M.D.; Esteve Ciudad, P.; Raigón Jiménez, M.D. The Effects of Low-Input (Wild and Organic Farming) Conditions on the Nutritional Profile of Ziziphus Jujuba Mill. Fruits from the Valencian Mediterranean. *Sustainability* **2023**, *15*, 14587. [CrossRef]
39. van Den Dool, H.; Dec. Kratz, P. A Generalization of the Retention Index System Including Linear Temperature Programmed Gas—Liquid Partition Chromatography. *J. Chromatogr. A* **1963**, *11*, 463–471. [CrossRef] [PubMed]
40. Singleton, V.L.; Rossi, J.A. Colorimetry of Total Phenolics with Phosphomolybdic-Phosphotungstic Acid Reagents. *Am. J. Enol. Vitic.* **1965**, *16*, 144–158. [CrossRef]
41. Bahorun, T.; Luximon-Ramma, A.; Crozier, A.; Aruoma, O.I. Total Phenol, Flavonoid, Proanthocyanidin and Vitamin C Levels and Antioxidant Activities of Mauritian Vegetables. *J. Sci. Food Agric.* **2004**, *84*, 1553–1561. [CrossRef]
42. Dence, C.W. *Moethods of Lignin Chemistry*; Springer: New York, NY, USA, 1992.
43. Sluiter, A.H.; Ruiz, B.; Scarlata, R.; Sluiter, C.; Templeton, J.; Crocker, D.D. *Determination of Structural Carbohydrates and Lignin in Biomass Laboratory Analytical Procedure*; NREL Report No. TP 510-42618; National Renewable Energy Laboratory: Golden, CO, USA, 2008.

Disclaimer/Publisher's Note: The statements, opinions and data contained in all publications are solely those of the individual author(s) and contributor(s) and not of MDPI and/or the editor(s). MDPI and/or the editor(s) disclaim responsibility for any injury to people or property resulting from any ideas, methods, instructions or products referred to in the content.